Transport in Porous Media (2023) 146:197–222
https://doi.org/10.1007/s11242-022-01793-5

Population Balance Models for Particulate Flows in Porous Media: Breakage and Shear-Induced Events

Matteo Icardi[1] · Nicodemo Di Pasquale[2] · Eleonora Crevacore[3] · Daniele Marchisio[4] · Matthaus U. Babler[5]

Received: 2 July 2021 / Accepted: 22 April 2022 / Published online: 26 May 2022

Abstract
Transport and particulate processes are ubiquitous in environmental, industrial and biological applications, often involving complex geometries and porous media. In this work we present a general population balance model for particle transport at the pore-scale, including aggregation, breakage and surface deposition. The various terms in the equations are analysed with a dimensional analysis, including a novel collision-induced breakage mechanism, and split into one- and two-particles processes. While the first are linear processes, they might both depend on local flow properties (e.g. shear). This means that the upscaling (via volume averaging and homogenisation) to a macroscopic (Darcy-scale) description requires closures assumptions. We discuss this problem and derive an effective macroscopic term for the shear-induced events, such as breakage caused by shear forces on the transported particles. We focus on breakage events as prototype for linear shear-induced events and derive upscaled breakage frequencies in periodic geometries, starting from nonlinear power-law dependence on the local fluid shear rate. Results are presented for a two-dimensional channel flow and a three dimensional regular arrangement of spheres, for arbitrarily fast (mixing-limited) events. Implications for linearised shear-induced collisions are also discussed. This work lays the foundations of a new general framework for multiscale modelling of particulate flows.

Keywords Population balance equation · Particulate flows · Upscaling · Mixing · Porous Media

✉ Matteo Icardi
Matteo.Icardi@nottingham.ac.uk

[1] School of Mathematical Sciences, University of Nottingham, Nottingham, UK

[2] Department of Chemical Engineering and Analytical Science, University of Manchester, Manchester, UK

[3] Dipartimento di Scienze Matematiche "G.L. Lagrange", Politecnico di Torino, Turin, Italy

[4] DISAT, Politecnico di Torino, Turin, Italy

[5] Department of Chemical Engineering, KTH Royal Insitute of Technology, SE-10044 Stockholm, Sweden

1 Introduction

The evolution of a population of particles can be described using the Population Balance Equation (PBE) (Ramkrishna 2000), which solves for the distribution of particle sizes in presence of phenomena such as breakup and aggregation. While the PBE framework was successfully applied in different chemical processes, such as the precipitation of polymer nanoparticles (Di Pasquale et al. 2012; Lavino et al. 2017; Lattuada et al. 2016), aggregation of colloids (Sadegh-Vaziri et al. 2018; Serra et al. 1997; Serra and Casamitjana 1998), or the description of foams and bubble evolution (Zitha and Du 2010; Buffo et al. 2012), limited works studying particulate processes in porous media, via the PBE, exist. While the PBE itself can be thought as a meso-scale description where the particles are described in a statistical ensemble conditioned on their size, it has wide applicability, thanks to its possible ramifications to different "scales". For example, we can describe the evolution of complex systems (e.g., polymer macromolecules) if we couple the PBE framework with microscopic modelling, such as Molecular Dynamics simulations (Di Pasquale et al. 2013, 2014) or discrete element methods (Frungieri et al. 2020); or we can couple its constituent terms (e.g. breakage and collision frequencies) with local flow properties obtained from Computational Fluid Dynamics (CFD) calculations (Di Pasquale et al. 2012; Lavino et al. 2017), obtaining a very precise description of the system considered.

In the presence of complex geometries and porous materials, the detailed resolution of the flow structures, while in principle possible (Marcato et al. 2021), it is often impractical and upscaled porous media models need to be introduced. While the derivation and calibration of single- and multi-phase flow and transport models have been widely studied in the porous media and fluid dynamics community Boccardo et al. (2017); Icardi and Dentz (2020), there is currently no general population balance theory at the Darcy/continuum scale. Krehel et al. (2015) studied the upscaling of a discrete number of particle sizes and derived upscaled equations in the assumption of slow aggregation kinetics. Several other authors (Won et al. 2021; Boccardo et al. 2019; Seetha et al. 2017) have studied the effect of poly-dispersity on transport and retention in porous media without including explicitly the particulate processes. Bedrikovetsky (2008) and subsequent works from the same authors developed micro- and macro-models based on discrete PBE concepts to explain various porous media phenomena but with no direct link to the pore-scale solution. Population balances have been applied at the Darcy-scale (Nassar et al. 2015; Patzek 1988) in a phenomenological way and parameters estimated experimentally.

The objective of this paper is, on one hand, to provide a thorough description of aggregation, breakage, and other particulate processes described by the PBE, while, on the other hand, laying the foundations of their multiscale analysis in heterogeneous and porous media. While the development of an effective macroscopic population balance model is the ultimate step, the starting point is the understanding of the fundamental processes and the emergent upscaled mechanisms. This is achieved by analysing the collision events and their dependence on particle and flow properties. To this aim, we provide, for the first time, a general dimensional analysis of all terms, including one- and two-particle processes, and we propose an upscaling methodology to extract macroscopic effective frequency kernels with a rigorous bottom-up approach.

Regarding the upscaling, in this work we limit ourselves to shear-induced breakage events in periodic media. A similar approach could also be applied for competitive events, considering multiple collision or breakage mechanisms. Similarly to the usual approach in population balance studies, the overall reaction rate (or collision kernel) can be

approximated as the sum of the contributions of the separate mechanisms. This is however not necessarily true for nonlinear (i.e. two-particle) events and when scales are not fully separable. Extensions of the upscaling methodology presented here, including nonlinear aggregation terms and more complex geometrical and physical models, are currently under development and will be subject of future investigations.

This paper is organised as follows. We first present a discussion of the PBE with particular emphasis on the aggregation and breakage mechanism, presented here in terms of single- and two-particles events. We will give a detailed derivation of the dimensional analysis of the PBE. We then move to describe the motion of a suspension of poly-dispersed particles through a porous medium filled with an incompressible fluid undergoing creeping-flow conditions, where we couple the non-dimensional PBE with the spatial averages over the pore domain. We then specialise the discussion to the breakage of the particle showing the relevant equations and derivations which include the collision models and the upscaling step. We then apply the framework we derived to two test cases, a two-dimensional channel flow and a three-dimensional face-centred cubic domain. We then presents some results and draw some conclusions.

2 Particulate Flow Model

Let us consider the motion of a suspension of a poly-dispersed population of particles through a porous medium, filled with an incompressible fluid, undergoing creeping-flow conditions. Let Ω be the fluid domain in a Representative Elementary Volume (REV) of a periodic porous medium, whose internal boundary is denoted as Γ.

While the flow through porous media can be described by the Darcy's equation, we start from the microscopic fluid dynamics description of an incompressible fluid in creeping flow conditions. Therefore, we introduce the dimensionless steady Stokes flow (with viscous scaling) (Auriault and Adler 1995):

$$\begin{aligned} \frac{\mu U}{PL}\Delta \boldsymbol{u} &= \nabla p \quad \text{in} \quad \Omega, \\ \nabla \cdot \boldsymbol{u} &= 0 \quad \text{in} \quad \Omega, \\ \boldsymbol{u} &= \mathbf{0} \quad \text{on} \quad \Gamma, \end{aligned} \tag{1}$$

where $\boldsymbol{u}$ is the (dimensionless) fluid velocity and p is the (dimensionless) pressure; μ is the viscosity, P, U, L are reference pressure, velocity and length, respectively. We consider a solid matrix composed of a collection of identical grains and choose the characteristic length to be equal to the grains diameter. No-slip conditions ($\boldsymbol{u} = 0$) are imposed on the grains surface Γ, while the other boundary conditions are not specified in 1 as they depend on the specific scenario.

Now, we consider the transport of a population of particles, described by the (dimensional) Particle Size Distribution (PSD) $\tilde{f}(\tilde{t}, \tilde{\mathbf{x}}, \tilde{m})$, in the pore space, that undergo aggregation, breakage and surface deposition. $\tilde{f}(\tilde{t}, \tilde{\mathbf{x}}, \tilde{m})$ represents the number density function of particles with mass within an infinitesimal interval around $\tilde{m}$ at the time $\tilde{t}$ in the position $\tilde{\mathbf{x}}$. We want to make a remark here that the PSD is usually written in terms of the dimensional particle size $\tilde{\ell}$. However, when binary interactions between particles are considered, it is more convenient to write such laws in terms of the mass, since, if we consider the aggregation of two particles of masses $\tilde{m}_1, \tilde{m}_2$ and sizes $\tilde{\ell}_1, \tilde{\ell}_2$, the resulting particle has mass $\tilde{m}_1 + \tilde{m}_2$ but it is not true in general that the final size is $\tilde{\ell}_1 + \tilde{\ell}_2$. The interaction laws such as collisions, between particles (e.g.,

Brownian collision, more on the next sections) are based on the particle size. However, this last fact does not represents a problem in our formulation, since we can always use the dimension of a particle $\tilde{\ell}$ described as a function of the mass $\tilde{m}$, i.e., $\tilde{\ell}(\tilde{m})$. Therefore, in our model we need to include the law describing the size of a particle given its mass. For a non-porous spherical particles with constant density $\tilde{\rho}$ such law is simply $\tilde{\ell}(\tilde{m}) = \sqrt[3]{\left(\frac{6\tilde{m}}{\tilde{\rho}\pi}\right)}$. In this work, the particle size, $\tilde{\ell}(\tilde{m})$, will always represents the diameter of a particle. We note here that with the definition of $\tilde{\ell}(\tilde{m})$ we considered, the non-dimensional particle length $\tilde{\ell}(m) = \mathfrak{l}\ell(\tilde{m})$, is given simply by $\ell(m) = \frac{\tilde{\ell}(\tilde{m})}{\mathfrak{l}} = \sqrt[3]{m}$ where we used the reference mass $\mathfrak{m}$ and reference length $\mathfrak{l}(\mathfrak{m}) = \sqrt[3]{\left(\frac{6\mathfrak{m}}{\tilde{\rho}\pi}\right)}$. However, we prefer to use in the equations presented in the next sections the term $\ell(m)$ instead of its explicit expression obtained here, $\sqrt[3]{m}$, to indicate that more general mass functions for the length can be used (e.g., in the case of fractal particles).

In order to avoid the definition of too many symbols, as a convention in this work, a symbol under the tilde ($\tilde{\cdot}$) represents a dimensional quantity. The same symbol without the tilde represents the non-dimensional version of the same quantity. We start by defining the following dimensionless quantities: a reference particle size $\mathfrak{l}$, a reference diffusion coefficients of the particles $\widetilde{D_0}$, and a reference distribution $\tilde{F}$. We note here that knowing the law connecting the mass of a particle and its size we can define a reference particle size or a reference particle mass. In this work we will work with the former. We note that, if $\tilde{f}$ represents the numerical distribution of the size of the particle per unit volume it has dimension of the inverse of a length to the power of four, i.e. $\left[\frac{1}{L^3\mathfrak{l}}\right]$. We note here that our problem therefore includes the definition of two different reference lengths, a "meso-scopic" one, referring to the pore-scale REV and a "micro-scopic" one referring to the particles. A third "macro-scopic" scale arises when averaging over the REV onto a larger continuum pore domain. In this work we focus on the micro- and meso-scales while we will obtain averaged quantities that can then be used at the macro-scale.

The evolution of $\tilde{f}(\tilde{t}, \tilde{\mathbf{x}}, \tilde{m})$ is described by the Population Balance Equation (PBE), which reads as (Marchisio and Fox 2013; Ramkrishna 2000):

$$\partial_{\tilde{t}}\tilde{f} + \tilde{\nabla}\cdot\left(\tilde{\boldsymbol{v}}\tilde{f}\right) - \widetilde{D}\widetilde{\Delta}\tilde{f} = \widetilde{A}\left(\tilde{f},\tilde{f},\tilde{m}\right) + \widetilde{B}_1\left(\tilde{f},\tilde{m}\right) + \widetilde{B}_2\left(\tilde{f},\tilde{f},\tilde{m}\right) \quad \text{in } \tilde{\Omega}\times(0,\infty)^2, \tag{2a}$$

$$\boldsymbol{n}\cdot\left(\tilde{\boldsymbol{v}}\tilde{f} - \widetilde{D}\widetilde{\nabla}\tilde{f}\right) = \widetilde{C}(\tilde{f},\tilde{m}) \quad \text{on } \tilde{\Gamma}\times(0,\infty)^2, \tag{2b}$$

where we dropped all the dependencies of $\tilde{f}$ for the sake of readability. The terms on the right-hand side of

Eq. (2) describe the particulate processes (aggregation, breakup, deposition) where the double appearance of $\tilde{f}$ in these terms indicates two-particle processes while, accordingly, the single appearance of $\tilde{f}$ indicates one-particle processes. Before describing in detail the different terms appearing in Eq. 2 we rewrite it in dimensionless form, dividing Eq. 2a by $\frac{\tilde{F}\widetilde{D_0}}{L^2}$ and Eq. 2b by $\frac{\tilde{F}\widetilde{D_0}}{L}$.

$$\begin{aligned} &\frac{\partial f}{\partial t} + \mathrm{Pe}\nabla\cdot(f\boldsymbol{v}) - D\Delta f = A + B_1 + B_2 \quad && \text{in } \Omega\times(0,\infty)^2, \\ &\boldsymbol{n}\cdot(\mathrm{Pe}\,\boldsymbol{v}f - D\nabla f) = C && \text{on } \Gamma\times(0,\infty)^2, \end{aligned} \tag{3}$$

Table 1 Definition of non-dimensional quantities used in the derivation of the PBE

$\tilde{f} = \tilde{F} f$	$\tilde{\boldsymbol{x}} = L\boldsymbol{x}$	$\tilde{t} = L^2 \widetilde{D_0}^{-1} t$
$\tilde{\boldsymbol{v}} = U\boldsymbol{v}$	$\widetilde{D} = \widetilde{D_0} D$	$\tilde{\ell} = \mathfrak{l}\ell$
$\widetilde{m} = \mathfrak{m} m$	$\widetilde{\nabla} = L^{-1}\nabla$	$\widetilde{\Delta} = L^{-2}\Delta$
$\frac{\partial}{\partial \tilde{t}} = \widetilde{D_0} L^{-2} \frac{\partial}{\partial t}$	$\widetilde{A} = F\widetilde{D_0} L^{-2} A$	$\widetilde{B}_1 = F\widetilde{D_0} L^{-2} B_1$
$\widetilde{B}_2 = F\widetilde{D_0} L^{-2} B_2$	$\widetilde{C} = F\widetilde{D_0} L^{-1} C$	$\mathrm{Pe} = UL\widetilde{D_0}^{-1}$

where we have used the non-dimensionalisation variables shown in Table 1. It is important to notice here that both the diffusion $\widetilde{D}$ and $\tilde{\boldsymbol{v}}$ may depend on particle size and therefore, after dividing by a reference diffusion coefficients and velocity (related to the reference particle size), both dimensionless functions D and $\boldsymbol{v}$ remain in the equation.

To obtain Eqs. 2 and 3, we have made the following modelling assumptions.

Particle velocity: $\boldsymbol{v}$ is the dimensionless velocity of particles of size $\tilde{\ell}$. We assume this to be a given function of both the velocity field $\mathbf{u}$ and the particle size, i.e., $\boldsymbol{v} = \boldsymbol{u} + \boldsymbol{u}_{\ell,\mathrm{rel}}$, where $\boldsymbol{u}_{\ell,\mathrm{rel}}$ is the slip velocity depending on the particle size. For small Stokes number we can use the approximated expression reported in (Ferry et al. 2003) for the relative velocity $\tilde{\boldsymbol{u}}_{\ell,\mathrm{rel}}$:

$$\tilde{\boldsymbol{v}} = \tilde{\mathbf{u}} + \tau(\tilde{\ell})\tilde{\mathbf{a}} \tag{4}$$

which can be rewritten in non-dimensional form as:

$$\boldsymbol{v} = \frac{\tilde{\boldsymbol{v}}}{U} = \frac{\tilde{\mathbf{u}}}{U} + \frac{\tau(\tilde{\ell})}{U}\tilde{\mathbf{a}} = \mathbf{u} + \frac{\mathrm{St}}{\mathrm{Fr}^2}\,\mathbf{a}\,\ell^2\,, \tag{5}$$

where $\tau(\tilde{\ell}) = \dfrac{\rho\tilde{\ell}^2}{18\mu}$ is the particle relaxation time (s), ρ is the density of the particle (kg m^{-3}), $\tilde{\mathbf{a}} = g\mathbf{a}$ is the particle acceleration (m s^{-2}) due to body forces, where $\mathbf{a}$ is the dimensionless unitary vector of the acceleration direction, $\mathrm{St} = \dfrac{\rho\mathfrak{l}^2}{18\mu}\dfrac{U}{L}$ is the Stokes number, and $\mathrm{Fr} = \sqrt{\dfrac{U^2}{Lg}}$ is the Froude number. The most common body forces considered is the gravity and therefore $\tilde{\mathbf{a}}$ is the gravity acceleration, but other body forces can be considered, e.g. electrostatic interactions. In this work we will also consider that the acceleration is the same (in magnitude and direction) for each particle.

Dilute limit: we assume the system is dilute, i.e., the overall volume fraction of the particles, which can be estimated as $F\mathfrak{l}^4$ (assuming the width of the distribution is of the same order of magnitude of the reference particle size), is large enough to have collisions between particles but small enough to assume particle momentum is independent from the concentration of particles and only dependent on particle Stokes number.

Particle diffusion: $D = \widetilde{D}(\tilde{\ell})/\widetilde{D_0}$ is the diffusivity ratio between particles of size $\tilde{\ell}$ and $\mathfrak{l}$. If we assume the Stokes-Einstein relation to compute the diffusion coefficient of spherical particles, i.e., $\widetilde{D}(\mathfrak{l}) = \dfrac{\kappa_B T}{3\pi\mu\mathfrak{l}}$, where κ_B is the Boltzmann constant (kg m^2 s^{-2} K^{-1}), and T the temperature (K), then the diffusivity ratio assume the simple form $D = \ell^{-1}$.

Particulate processes: $A(\tilde{f},\tilde{f},\widetilde{m})$, $B_1(\tilde{f},\widetilde{m})$, $B_2(\tilde{f},\tilde{f},\widetilde{m})$ are the dimensionless functions describing aggregation, single particle breakage, and two particles breakage, respectively. In the literature on the PBE, the source term is often written in terms of death and birth rates, which both includes aggregation and breakage terms (Ramkrishna 2000), e.g. an aggregation event can lead to the birth of a new particle of size $\tilde{\ell}$ or the death of a particle

of that size. In this work, however, we are interested in analysing the source term in terms of particle events, for which the division in aggregation and breakage looks more clear. The description of the single or double particles events will be the main topic of next sections. We want to highlight here that the functions themselves are dimensionless, but they still depend on dimensional arguments (i.e. $\tilde{f}$ and $\tilde{\ell}$). In the next section will rewrite these functions in terms of dimensionless arguments.

Particle deposition: The boundary term $C(\tilde{f}, \widetilde{m})$ represents the particle deposition on the surface of the porous matrix, described as a generic flux. This is an important process, highly dependent on particle size, but often neglected in PBE models and it appears as a boundary condition on Γ in Eq. 2 (and accordingly in Eq. 3) to take into account the modification of the PSD due to particle deposition on the surface of the porous matrix. In other words, the flux (convective and diffusive) of the particles normal to the interface, equals the ones deposited on the surface given by the deposition kinetic described through the function $C(\tilde{f}, \widetilde{m})$.

In the following we will often indicate the processes of aggregation, breakage and surface deposition mechanisms with the collective name of *reactions* even though no chemical reactions are involved. We decided for this extended use of the word *reactions* to allow a more general mathematical treatment of the upscaling mechanisms by using effective Damköhler number as the ratio between the reaction rate and the diffusive mass transport rate (Bird et al. 2002). The occurrence of this term in the following must be intended with this extended use in mind.

3 Particulate Processes

In this section we will perform a dimensional analysis of the different phenomena experienced by a particle. In turn, this analysis will allow us to properly define the source terms in Eq. 3 in terms of dimensionless quantities only. The most straightforward classifications of such events consider the number of particles involved. Here, we assume that events including more than three-particles are so rare that can be neglected. Therefore, in this analysis we will focus on one- and two-particles events.

While the aggregation depends on the collision frequency between two particles and the probability of the collision to be effective, for the breakage we can distinguish between single particle and two particles events instead. We call the former processes "linear reactions" and the latter ones "nonlinear reactions". Breakup caused by interaction of particles can be due to impacts of particles (Chen and Li 2020; Khalifa and Breuer 2021) but also due to viscous shear stresses generated when particles come close (Frungieri and Vanni 2021). Part of our analysis will include the dimensional analysis of the terms appearing inside the source components in Eq. 3 and rewriting these contributions as non-dimensional quantities. This, in turn, will lead to the definition of another non-dimensional number, an equivalent Damköhler number, as the ratio between reaction and diffusion time scales. We represented a sketch of the different mechanism we are considering here in Fig. 1.

3.1 Single-Particle Events: Shear-Induced Interactions

Single-particle events can be induced by different mechanism, such as local shear rate, or collisions with the walls. Let us consider shear-induced events and a threshold force,

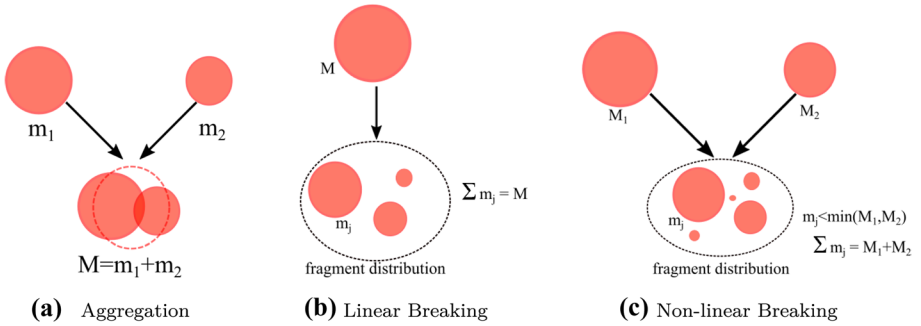

Fig. 1 Sketch of the particle interactions considered in this paper. From left to right, aggregation of two particles of mass m_1 and m_2 generates a particle of mass $M = m_1 + m_2$; the breakage of a particle of mass M generates a distribution of fragments of mass $m_j < M$ with $\sum m_j = M$; the collision of two particles of mass M_1 and M_2 creates a distribution of particles such that their size $m_j < \min(M_1, M_2)$ and $\sum m_j = M_1 + M_2$

which we call the *critical* force, $\mathcal{F}_{cr}$, which represents the average force needed to break the aggregate. Having described breakage events in a statistical way, we can therefore express the breakage frequency $\tilde{\beta}$ as:

$$\tilde{\beta} = \tilde{B}'_0 \left(\frac{\mathcal{F}}{\mathcal{F}_{cr}} \right)^{\gamma} \tag{6}$$

where $\mathcal{F}$ is the force acting on the aggregates and $\tilde{B'}_0$ is the characteristic breakup frequency (s^{-1}) for the reference particle size. The parameter $\gamma \geq 0$ controls how likely is for a particle experiencing a force larger than the critical force to break. For large γ, the frequency of breakage below the critical force is negligible while it becomes very large for larger forces. In the limit of small γ, instead, the breakage is a constant independent random event. The law reported in Eq. 6 is the same power law reported in the literature (Barthelmes et al. 2003) having recognised the role played by the shear stress into this process. The critical force needed to break an aggregate should depend on the size of the aggregate itself. The evidence suggest that in the presence of shear big particles broke easily than small ones (Serra and Casamitjana 1998). We assume therefore for the critical force that $\mathcal{F}_{cr} = \mathcal{F}_0 \ell^{-\eta}$, where $\mathcal{F}_0$ is the reference force defined as the force needed to break a reference particle of size $\mathfrak{l}$ and $\eta > 0$ is a parameter. Let us rewrite Eq. 6 as:

$$\tilde{\beta} = \tilde{B}_0 \left(\frac{\mu \tilde{\sigma} \tilde{\ell}^2}{\mathcal{F}_0 \ell^{\eta}} \right)^{\gamma} = \tilde{B}_0 \left(\frac{\mu U \mathfrak{l}^2}{L \mathcal{F}_0} \right)^{\gamma} \ell^{\gamma'} \sigma^{\gamma} = \tilde{B}_0 \Theta \beta \tag{7}$$

where we have estimated the average force on the particle as $\mathcal{F} \propto \mu \tilde{\sigma} \tilde{\ell}^2$, proportional to viscous stresses and particle surface area, and where we have defined the new dimensionless number $\Theta = \left(\frac{\mu U \mathfrak{l}^2}{L \mathcal{F}_0} \right)^{\gamma}$, a dimensionless kernel $\beta = \ell^{\gamma'} \sigma^{\gamma}$, and $\gamma' = \gamma(2 - \eta)$. Herein, we assume $\eta = 2$ (i.e. critical force proportional to the surface area) and therefore $\gamma' = 0$.

In Eq. 7, the shear rate $\tilde{\sigma}$ is calculated as

$$\tilde{\sigma}(\boldsymbol{x}) = \left\| \frac{1}{2} \left(\nabla \mathbf{u}(\boldsymbol{x}) + (\nabla \mathbf{u}(\boldsymbol{x}))^{\mathrm{T}} \right) \right\| \tag{8}$$

where $\|\cdot\|$ is the Frobenius norm and $(\cdot)^{\mathrm{T}}$ is the transpose of the argument. Here, we emphasised the fact that $\tilde{\sigma}$ depends on the position, but in the rest of the work we drop the spatial dependence to simplify the notation. Another possibility, to have more consistent and comparable results for large different γ and highly heterogeneous shear rates, we can normalise the shear by its gamma-moment, $\langle\sigma^{\gamma}\rangle$ (where $\langle\cdot\rangle$ is the average operator), resulting in the dimensionless kernel

$$\beta = \ell^{\gamma'} \frac{\sigma^{\gamma}}{\langle\sigma^{\gamma}\rangle} \tag{9}$$

with constant $\tilde{B}_0\langle\sigma^{\gamma}\rangle\Theta$ and effective Damköhler number $\mathrm{Da}_{\beta} = \frac{\tilde{B}_0\langle\sigma^{\gamma}\rangle L^2}{\widetilde{D_0}}\Theta$.

3.2 Two-Particle Events

When two-particle collide in a fluid, different mechanisms are involved, which can depend on the movement of the fluid itself. For this reason, two-particle collision events are described as a sum of single mechanism, and the decisions on which ones are to be included depends on the particular problem we are considering.

In this work we will focus on the Brownian, shear and settling velocity mechanism, even though others are available, such as the turbulent mechanism (Di Pasquale et al. 2012; Lavino et al. 2017). For each mechanism we define a constant, which we will indicate with K_X with X related to the particular mechanism considered, which collect all the dimensional reference quantities as well as the multiplicative coefficients for each mechanism. In turn, this constant divided by the reference volume will represents the *characteristic frequency* of the particular mechanism (with dimension 1/s). The two-particles events described by collision mechanisms are defined in terms of the particle size. However, as explained in appendix 2, the particle size is assumed to be a known function of the mass of the particles. That is to say that we can write for the generic (dimensional) collision kernel $\tilde{\alpha}_X(\tilde{\ell}(\tilde{m}_i), \tilde{\ell}(\tilde{m}_j))$, where $\tilde{m}_i$ and $\tilde{m}_j$ are the masses of two generic particles. In order to light the notation, in the next sections we will drop the mass dependence and write $\tilde{\alpha}_X(\tilde{\ell}_i, \tilde{\ell}_j)$ if it is clear from the context to what we are referring to. However, in general the mass dependence is always implied when the size of a particle $\tilde{\ell}$ is considered.

For two-particle events, the Damköhler number is defined as $\mathrm{Da}_{\mathrm{X}} = K_X F \frac{L^2 \mathfrak{m}}{\widetilde{D_0}}$. K_X is the process constant and its exact definition depends on the particular process considered. There will be therefore several Damköhler numbers, one for each mechanism and they will be distinguished by using the same subscripts we used for the process constants.

Assuming spherical particles of diameter $2\tilde{\ell}$, and considering only the rectilinear approximation of particle encounters[1], it is possible to discriminate which is the leading collision mechanism in the following way (Serra et al. 1997):

- Brownian motion for $\tilde{\ell} < 1\mu$m, with a (dimensional) collision frequency between particle of diameters $\tilde{\ell}$ and $\tilde{\ell}_i$

[1] the more accurate curvilinear approximation can be used by adding a correction factor, typically particle size dependent, in front of the rectilinear collision frequency

$$\tilde{\alpha}_{\mathrm{B}}(\tilde{\ell},\tilde{\ell}_i) = 2\pi\left(\tilde{\ell}+\tilde{\ell}_i\right)\left(\widetilde{D}(\tilde{\ell})+\widetilde{D}(\tilde{\ell}_i)\right) \tag{10}$$

In dimensionless form, assuming particles with constant density, this is equivalent to

$$\tilde{\alpha}_{\mathrm{B}}(\tilde{\ell},\tilde{\ell}_i) = 2\pi\widetilde{D_0}\mathfrak{l}\left(\ell+\ell_i\right)\left[D+D_i\right] = 2\pi\widetilde{D_0}\mathfrak{l}\alpha_{\mathrm{B}}(\ell,\ell_i) = K_{\mathrm{B}}\alpha_{\mathrm{B}}(\ell,\ell_i) \tag{11}$$

where we defined the Brownian constant $K_{\mathrm{B}} = \widetilde{D_0}2\pi\mathfrak{l}$.

- Shear stress for $1\mu\mathrm{m} < \tilde{\ell} < 40\mu\mathrm{m}$, with

$$\tilde{\alpha}_{\mathrm{S}}(\tilde{\ell},\tilde{\ell}_i) = \tfrac{1}{6}(.)\tilde{\ell}+\tilde{\ell}_i{}^3\tilde{\sigma}$$

from which we obtain:

$$\begin{aligned}\tilde{\alpha}_{\mathrm{S}}(\tilde{\ell},\tilde{\ell}_i) &= \frac{U\mathfrak{l}^3}{L}\left(\ell+\ell_i\right)^3\sigma \\ &= \frac{U\mathfrak{l}^3}{L}\alpha_{\mathrm{S}}(\ell,\ell_i) = K_{\mathrm{S}}\alpha_{\mathrm{S}}(\ell,\ell_i)\,.\end{aligned} \tag{12}$$

We here defined the shear stress constant $K_{\mathrm{S}} = \frac{U\mathfrak{l}^3}{6L}$.

- Differential settling for $\tilde{\ell} > 40\mu\mathrm{m}$, it can written as:

$$\tilde{\alpha}_{\mathrm{D}}(\tilde{\ell},\tilde{\ell}_i) = \frac{\pi}{4}\left(\tilde{\ell}+\tilde{\ell}_i\right)^2\left|\tilde{\boldsymbol{v}}-\tilde{\boldsymbol{v}}_i\right| \tag{13}$$

and by considering Eq. 4, we have:

$$\begin{aligned}\tilde{\alpha}_{\mathrm{D}}(\tilde{\ell},\tilde{\ell}_i) = = \frac{\pi U\mathfrak{l}^2}{4}\left(\ell+\ell_i\right)^2\left|\boldsymbol{v}-\boldsymbol{v}_i\right| \\ = \frac{\pi U\mathrm{St}\mathfrak{l}^2}{4\mathrm{Fr}^2}\left(\ell+\ell_i\right)^2\left|\mathbf{a}\ell^2-\mathbf{a}\ell_i^2\right| \\ = \frac{\pi U\mathrm{St}\mathfrak{l}^2}{4\mathrm{Fr}^2}\alpha_{\mathrm{D}}(\ell,\ell_i) \\ = K_{\mathrm{D}}\alpha_{\mathrm{D}}(\ell,\ell_i)\end{aligned} \tag{14}$$

with a constant equal to $K_{\mathrm{D}} = \frac{\pi\mathrm{St}U\mathfrak{l}^2}{4\mathrm{Fr}^2}$.

It is worth highlighting here that these two-particles mechanisms conserve the total mass. This observation is important and is preserved at a discrete level when, for example, the PBE is solved with the method of moments (for a more detailed account of the Method of Moments see (Marchisio and Fox 2013)).

3.3 Aggregation and Breakage Models

In the literature on the PBE, two terms are usually defined to describe the aggregation and breakage, α and β which are known as the aggregation and breakage kernels (frequencies) respectively (Marchisio and Fox 2013). However, in this work we want to present a different interpretation of the aggregation kernel as a term not related only to the aggregation but more in general as an interaction term between two particles (we remind here that we assumed that three or more particle events are negligible). The interaction between particles must be understood only as a collision and therefore in this work α represents the collision kernel which

we analysed in the previous sections (see Sect. 3.2), where we gave explicit definition of the Brownian, Shear and Differential Settling mechanisms. In turn, this collision can create a bigger aggregate (aggregation) or breaks the particles into smaller ones (breakage). In the literature, the breaking mechanism is usually described as one particle process, where the particle breaks either because of its interaction with the fluid flow in which it is immersed (e.g. Turbulent stresses, Viscous shear stresses, Shearing-off processes) (Solsvik et al. 2013) or for its own interfacial instabilities (Solsvik et al. 2013). This description comes from the main application of the PBE in the past years, bubbles and drops. In this case, the only effect of the collision of two bubbles (or drops) is their coalescence into a new bubble (aggregation). For (solid) particles the previous is not true. The collision between two particles can either create a bigger aggregate, if their structure allows them (e.g. for polymers Di Pasquale et al. (2012, 2013)), or they can break because of the collision, or nothing happen. Therefore, in this formulation we will describe two-particle events leading to an aggregation, and two-particle events leading to a breakage. Of course, there is still the possibility that particles collide without aggregation or breaking.

In order to distinguish among these three possibilities (aggregation, breakdown, or nothing) we define two new parameters κ_A and κ_B, the former represents the probability that a collision leads to aggregation, the latter is the probability that a collision event leads to breakage. We note that κ_B and κ_A can be considered as the efficiency of aggregation and breakage, respectively. Being defined as efficiencies then $0 \leq \kappa_A \leq 1$, and the same for κ_B. We can distinguish two possible scenarios:

- if $\kappa_B + \kappa_A = 1$, then we assume that each collision event is going to lead either to an aggregation or to a breakage.
- if $\kappa_B + \kappa_A < 1$, a collision event has one result among these three events: an aggregation, a breakage or nothing.

It can be easily seen that each possible special cases is included by choosing particular values for κ_A and κ_B, e.g., if we assume $\kappa_A = 1$ then each and every collision will result in an aggregation (see e.g. (Di Pasquale et al. 2012)).

We start our analysis by considering the aggregation $A(\tilde{f}, \tilde{f}, \tilde{\ell})$ term in Eq. 3. This latter object can be considered a functional with respect the PSD, and a function with respect the particle size ℓ. It can be described as follow, where we note that the dependence on time and space variables have been dropped for the sake of legibility (Vanni 2000; Serra and Casamitjana 1998):

$$A(\tilde{f}, \tilde{f}, \tilde{m}) = \sum_X A_X^-(\tilde{f}, \tilde{f}, \tilde{m}) + \sum_X A_X^+(\tilde{f}, \tilde{f}, \tilde{m}) \tag{15}$$

here, the sums run over the different mechanisms described in appendix 3, i.e. $X \in \{B, S, D\}$. The two terms in Eq. 15 represent, respectively, the creation of particles of size $\tilde{\ell}$, and the disappearing of particle of size $\tilde{\ell}$ both following an aggregation event.

Writing explicitly the first term, including the adimensionalisation constant $\frac{L^2}{\widetilde{D_0}\tilde{F}}$ (see Eq. 3), we have:

$$\begin{aligned}\frac{L^2}{\widetilde{DF}}\tilde{A}_X^-(\tilde{f},\tilde{f},\widetilde{m}) &= -\frac{L^2}{\widetilde{D_0F}}\int_0^{+\infty}\kappa_A\tilde{\alpha}_X(\tilde{\ell}(\widetilde{m}),\tilde{\ell}(\widetilde{m}_i))\tilde{f}\tilde{f}_i\,\mathrm{d}\,\widetilde{m}_i\\ &= -\frac{L^2}{\widetilde{D_0F}}\int_0^{+\infty}\kappa_A K_X\alpha_X(\ell(m),\ell(m_i))\,FfFf_i\mathfrak{m}\,\mathrm{d}\,m_i\\ &= -\mathrm{Da}_X f\int_0^{+\infty}\kappa_A\alpha_X(\ell(m_i),\ell)f_i\,\mathrm{d}\,m_i = \mathrm{Da}_X A_X^-(f,f_i,m).\end{aligned} \tag{16}$$

where α_X represents one of the interaction kernels defined above, and the subscript X refers to the fact that one or more of those mechanism can be included, depending on the particular problem considered, Da_X is the Damköhler number for the aggregation referring to the particular process X, κ_A is the probability that a collision leads to an aggregation and $\tilde{f}_i$ is a shorthand notation for $\tilde{f}(\widetilde{m}_i)$. $A^-(\tilde{f},\tilde{f},\widetilde{m})$ represents the reduction of the population of particles of mass m due to their aggregation with any other particle. For the second term in Eq. 15 we can write, with a derivation similar to the one shown in Eq. 16:

$$\frac{L^2}{\widetilde{DF}}\tilde{A}_X^+(\tilde{f},\tilde{f},\widetilde{m}) = \mathrm{Da}_X A_X^+(f,f,m) = \mathrm{Da}_X\frac{1}{2}\int_0^m\kappa_A\alpha_X(\ell(m_i),\ell(m-m_i))f(m_i)f(m-m_i)\,\mathrm{d}\,m_i\,. \tag{17}$$

$\tilde{A}^+(\tilde{f},\tilde{f},\widetilde{m})$ represents the (dimensional) increase in the number of particle of mass m due to aggregation of a particle of mass $m_i < m$ and $m - m_i$, whereas $A^+(\tilde{f},\tilde{f},\widetilde{m})$ is its non-dimensional version.

In the case of breaking, we have two different terms to consider, namely $\tilde{B}_1$ and $\tilde{B}_2$, representing the single particle and the two particle events, respectively. As we did for the aggregation case, we need to distinguish between two different occurrences in which a new particle of mass $\widetilde{m}$ is created by a breakage, or a particle of mass $\widetilde{m}$ is destroyed by the breakage. However, the breakage mechanism, differently from the aggregation one, contains a further term in its formulation, the so-called daughter distribution function, $\tilde{\mathcal{A}}(\widetilde{m}_i,\widetilde{m})$.

When a particle with mass $\widetilde{m}_i > \widetilde{m}$ breaks it can produce a range of fragments (with the obvious constraints that no fragment can be greater both in mass or in size than the original one). In our formulation we need to keep track of this effect to include in our count all the new fragments with size $\ell(m)$ created. It turns out that it is convenient to redefine the daughter distribution function $\tilde{\mathcal{A}}(\widetilde{m}_i,\widetilde{m})$ as:

$$\tilde{\mathfrak{A}}(\widetilde{m}_i,\widetilde{m}) = \tilde{\mathcal{A}}(\widetilde{m}_i,\widetilde{m}) - \tilde{\delta}(\widetilde{m}_i - \widetilde{m}) \tag{18}$$

where $\tilde{\delta}$ is the Dirac delta-function. We can observe that the new generalised daughter distribution function $\tilde{\mathfrak{A}}(\widetilde{m}_i,\widetilde{m})$ has the right measures of the inverse of a mass. The two terms in Eq. 18 take into account the fact that the breaking of a particle of size $\widetilde{m}_i > \widetilde{m}$ can increase the population of particles with mass $\widetilde{m}$, whereas the breaking of a particle with mass $\widetilde{m}$ always decreases the population of such particles.

The single particle events B_1 is now given by:

$$\begin{aligned}\frac{L^2}{\widetilde{D_0F}}\tilde{B}_1(\tilde{f},\widetilde{m}) &= \frac{L^2}{\widetilde{D_0F}}\int_{\widetilde{m}}^{+\infty}\tilde{\mathfrak{A}}(\widetilde{m}_i,\widetilde{m})\,\tilde{\beta}(\widetilde{m}_i)\tilde{f}(\widetilde{m}_i)\,\mathrm{d}\,\widetilde{m}_i\\ &= \frac{\tilde{B}_0\langle\sigma^\gamma\rangle L^2}{\widetilde{D_0}}\Theta\int_m^{+\infty}\mathfrak{A}(m_i,m)\,\beta(m_i)f(m_i)\,\mathrm{d}\,m_i = \mathrm{Da}_\beta B_1(f,m).\end{aligned} \tag{19}$$

Table 2 Definition of the dimensionless relevant quantity for the study of the breakage and aggregation problem

Particulate process, X	Frequency Kernel	Characteristic Frequency	Damköhler Number (diffusive)	Damköhler Number (convective)
		K	Da_X	$\mathrm{Da}_\mathrm{X}^{II}$
Two-particle events (aggregation or breakage)				
Brownian motion, B	$\left(\ell_j+\ell_i\right)\left[D_j+D_i\right]$	$2\pi\widetilde{D_0}\mathfrak{l}$	$2\pi F(\mathfrak{l}L)^2$	$2\pi F\dfrac{\widetilde{D_0}}{U}\mathfrak{l}^2L$
Shear, S	$\left(\ell_i+\ell_j\right)^3\sigma$	$\dfrac{1}{6}\dfrac{\mathfrak{l}^3U}{L}$	$\dfrac{1}{6}F\mathrm{Pe}\,\mathfrak{m}\mathfrak{l}^3$	$\dfrac{1}{6}F\,\mathfrak{m}\mathfrak{l}^3$
Differential settling, D	$\left(\ell_i+\ell_j\right)^2\lvert\ell_i^2-\ell_j^2\rvert$	$\dfrac{\pi}{4}\dfrac{\mathfrak{l}^2U\mathrm{St}}{\mathrm{Fr}^2}$	$\dfrac{\pi}{4}\dfrac{\mathrm{StPe}}{\mathrm{Fr}^2}F\mathfrak{m}\mathfrak{l}^2L$	$\dfrac{\pi}{4}\dfrac{\mathrm{St}}{\mathrm{Fr}^2}F\mathfrak{m}\mathfrak{l}^2L$
Single-particle events (breakage)				
Shear, $\Theta=\left(\frac{\mu U\mathfrak{l}^2}{L\mathcal{F}_0}\right)^\gamma$	$\ell^{\gamma'}\frac{\sigma^\gamma}{\langle\sigma^\gamma\rangle}$	$\tilde{B}_0\langle\sigma^\gamma\rangle\Theta$	$\dfrac{\tilde{B}_0\langle\sigma^\gamma\rangle L^2}{\widetilde{D_0}}\Theta$	$\dfrac{\tilde{B}_0\langle\sigma^\gamma\rangle L}{U}\Theta$

where $\mathfrak{A}(m_i,m)=\mathfrak{m}\tilde{\mathfrak{A}}(m_i,m)$, and we included the non-dimensional number Θ in the definition of Da_β.

The formulation of two-particle events for breakage is different from the ones shown for aggregation, because here either of the two particles involved in the collision can break, leading to:

$$\tilde{B}_X(\tilde{f},\tilde{f},\widetilde{m})=\int_{\widetilde{m}}^{+\infty}\int_0^{+\infty}\kappa_B\left(\tilde{\mathfrak{A}}(\widetilde{m}_i,\widetilde{m})+\tilde{\mathfrak{A}}(\widetilde{m}_j,\widetilde{m})\right)\tilde{\alpha}_X(\tilde{\ell}_i,\tilde{\ell}_j)\tilde{f}(\widetilde{m}_i)\tilde{f}(\widetilde{m}_j)\,\mathrm{d}\,\widetilde{m}_i\,\mathrm{d}\,\widetilde{m}_j\,. \tag{20}$$

where X represents the collision mechanism, we have assumed that each particle breakup event is independent and the breakup frequency κ_B is constant with respect to the particle size. Its non-dimensional versions is given by:

$$\begin{aligned}\frac{L^2}{\widetilde{D_0}F}\tilde{B}_X(\tilde{f},\tilde{f},\widetilde{m})&=\frac{L^2}{\widetilde{D_0}F}\int_m^{+\infty}\int_0^{+\infty}\kappa_B\frac{1}{\mathfrak{m}}\left(\mathfrak{A}(\widetilde{m}_i,\widetilde{m})+\mathfrak{A}(\widetilde{m}_j,\widetilde{m})\right)K_X\alpha_X(\ell_i,\ell_j)F\tilde{f}(\widetilde{m}_i)Ff(\widetilde{m}_j)\mathfrak{m}^2\,\mathrm{d}\,m_i\,\mathrm{d}\,m_j\\&=\frac{L^2K_XF\mathfrak{m}}{\widetilde{D_0}}\int_m^{+\infty}\int_0^{+\infty}\kappa_B\left(\mathfrak{A}(m_i,m)+\mathfrak{A}(m_j,m)\right)\alpha_X(\ell_i,\ell_j)\tilde{f}(m_i)f(\widetilde{m}_j)\,\mathrm{d}\,m_i\,\mathrm{d}\,m_j\\&=\frac{L^2K_XF\mathfrak{m}}{\widetilde{D_0}}B_X(f,f,m)=\mathrm{Da}_\mathrm{X}B_X(f,f,m)\,.\end{aligned} \tag{21}$$

We note here an important symmetry between aggregation and two-particle events breaking, the Damköhler number is the same for both of them, its only dependence is on the particular two-particle collision mechanism (represented by the subscript X).

Now we are in the position to show explicitly the Damköhler number for the different mechanism in Sect. 3.2. We obtain for each mechanism:

- Brownian motion: $\mathrm{Da_B} = 2\pi \mathfrak{l} \widetilde{D_0} \dfrac{FL^2\mathfrak{m}}{\widetilde{D_0}} = 2\pi F \mathfrak{l} \mathfrak{m} L^2$.
- Shear stress: $\mathrm{Da_S} = \dfrac{U\mathfrak{l}^3}{6L} \dfrac{FL^2\mathfrak{m}}{\widetilde{D_0}} = \dfrac{1}{6} F\mathrm{Pe}\, \mathfrak{m}\mathfrak{l}^3$.
- Differential Settling: $\mathrm{Da_D} = \dfrac{\pi \mathrm{St} U\mathfrak{l}^2}{4\mathrm{Fr}^2} \dfrac{FL^2\mathfrak{m}}{\widetilde{D_0}} = \dfrac{\pi}{4} \dfrac{\mathrm{StPe}}{\mathrm{Fr}^2} F\mathfrak{m}\mathfrak{l}^2 L$.

Table 2 summarises this convenient dimensionless formulation, and will allow us to significantly simplify the parametric sweeping and analysis of the macroscopic rate of collision/breakage events in the next section.

3.4 Particle Deposition

We provide here a short description of the particle deposition mechanism C in Eq. 24. A more detailed analysis of this term and its interactions with the aggregation/breakage processes will be subject of future works.

The deposition term C in Eq. 24, is a simple, yet general, way of incorporating several deposition mechanisms into a single (effective, meso-scale) boundary condition, relating the flux at the boundary with a deposition kinetics. It is common to include in the fluxes only the diffusion term (see e.g., (Grigoriev et al. 2020; Boccardo et al. 2017), assuming therefore a zero velocity of the particles at the wall. This is true only for solute or very small particles, while, as we have seen in Eq. 4, inertial particles can have a nonzero velocity at the boundary due to, for example gravity or electrostatic attractions. It is recommended, therefore, to write a more general boundary condition including also the convective fluxes.

We assume that the deposition mechanism can be described as a first-order, possibly nonlinear, irreversible kinetics:

$$\tilde{C} = \tilde{k}_c(\tilde{\ell})\tilde{f} \tag{22}$$

where $\tilde{k}_c(\tilde{m}) < 0$ is the deposition constant as a function of the particle mass. For example, steric deposition (deposition due to the finite size of the particles colliding into the solid) can be estimated to be $\propto r^a$ with $a \leq 1$. Other deposition mechanisms (chemically or electrostatic-induced) might have in general a positive or negative a. It is important to notice that we consider here only deposition as irreversible so detachment is not contemplated.

In the case of no deposition $\tilde{k}_c = 0$ and Eq. 2b represents simply a (Robin- or Neumann-type) boundary condition stating that the total flux of particles onto the boundary is zero. In the case of infinitely fast (i.e., perfect) deposition, each particle arriving on the boundary deposits instantaneously and are no longer in the system. This means that there are no "free" particles on Γ and we obtain the homogeneous Dirichlet boundary condition $\tilde{f} = 0$ on Γ. Simple extensions for reversible linear deposition are also possible by adding an additional balance equation for deposited particles and will be explored in further work.

The non-dimensional version of Eq. 2b can be written again as:

$$C = \mathrm{Da_c} k_c(m) f \tag{23}$$

where $k_c(m)$ is the non-dimensional deposition constant rate, and $\mathrm{Da_c}$ is the reaction coefficient for the deposition events, (Damköhler number for the deposition). The explicit

definition of Da_c depends on the specific deposition mechanism and will be considered in details in future publications.

4 Upscaling

The final form of the dimensionless PBE derived in the previous section reads as follows:

$$\begin{aligned}
&\frac{\partial f}{\partial t} + \mathrm{Pe}\nabla\cdot(f\boldsymbol{v}) - D\Delta f = \\
&\quad \sum_X \mathrm{Da}_X \left[\frac{1}{2}\int_0^m \kappa_A \alpha_X(\ell(m), \ell(m-m_i)) f(m_i) f(m-m_i)\,\mathrm{d}\,m_i - f\int_0^{+\infty} \kappa_A \alpha_X(\ell, \ell_i) f_i\,\mathrm{d}\,m_i \right. \\
&\quad \left. + \int_0^{+\infty} \kappa_B\big(\mathfrak{A}(m_i,m) + \mathfrak{A}(m_j,m)\big)\,\alpha_X(\ell_i,\ell_j) f(m_i) f(m_j)\,\mathrm{d}\,m_i\,\mathrm{d}\,m_j \right] + \mathrm{Da}_\beta \int_m^{+\infty} \mathfrak{A}(m_i,m)\,\beta(\ell_i) f(m_i)\,\mathrm{d}\,m_i
\end{aligned} \tag{24}$$

with boundary conditions

$$\boldsymbol{n}\cdot(\mathrm{Pe}\,\boldsymbol{v}f - D\nabla f) = \mathrm{Da}_c k_c(m) f \ .$$

The detailed analysis and resolution of the different terms (aggregation, breakage, and deposition) in Eq. 24 depends critically on the specific system, and in particular, on their dynamics with respect the typical time scales of the evolution of the flow in the system under study. In order to quantify these differences, we can use the Damköhler and the Pe, and we can distinguish three different regimes.

When $\mathrm{Da} \ll \mathrm{Pe}$, we can assume that the breakage, aggregation and deposition processes are slower than mixing. This latter fact, in turn, means that we can safely neglect both the interactions between these processes and the secondary collision events. The upscaled reactions can be trivially transferred from micro- to macro-scale as they are not mixing-limited. This is the case studied with periodic homogenisation by Krehel et al. (2015) and it can be shown that the same applies also to nonlinear rates.

When $\mathrm{Da} \approx \mathrm{Pe}$, the effective reactions (i.e. microscopically caused by average frequency of particle encounters) start to be significantly affected by advection patterns and influence effective upscaled velocity and dispersion. In particular, the effective reaction rate is no more linearly dependent on the microscopic reaction/collision rate. Nonlinearities, in general, can be upscaled only locally. Furthermore, poly-dispersity starts to play an important role, as successive collisions can happen within the same upscaling averaging volume.

Finally, when $\mathrm{Da} \to \infty$ mixing-limited asymptotic behaviours can be identified for the reaction rate. When the reaction happens only on a sub-domain or lower dimensional manifold, this saturates to a Péclet-dependent constant reaction rate (Boccardo et al. 2017), while, if the reaction (although heterogenous) happens in the whole domain, we expect the effective reaction rate to grow to infinity as it is limited but not completely impeded by the incomplete mixing.

Applying this principle to the PBE Eq. 24, and using the dimensionless numbers in Table 2, we can find the conditions that ensure the system is well mixed, and therefore processes (including the nonlinear ones) can be decoupled and upscaled with a effective macroscopic constant, proportional to the pore-scale one. The conditions on the reference number density and particle size are

$$
\begin{aligned}
F\mathfrak{l}^2 &< \frac{U}{2\pi\widetilde{D_0}L}\,,\\
F\mathfrak{l}^4 &< 6\,,\\
F\mathfrak{l}^3 &< \frac{4\mathrm{Fr}^2}{\pi\mathrm{St}L}\,,\\
\mathfrak{l}^2 &< \frac{L\mathcal{F}_0}{\mu U}\left(\frac{U}{L\tilde{B}_0}\right)^{1/\gamma}.
\end{aligned}
$$

It is important to recall that, although the constraint for shear-induced breakage does not explicitly involve the reference number density F, we have assumed that the system is dilute. The second constraint, coming from shear-induced collisions is similar, as expected, to the dilute limit approximation.

In case of wide particle size distributions, where the minimum and maximum particle size are orders of magnitude different from the reference particle size, the distinction above is not valid for all particles and a robust upscaling procedure, valid for all cases, should be considered. This will be the aim of our future works.

4.1 Formal Averaging and Closure Problems

Let us define the following (static) volume averaging operators:

$$
\langle\cdot\rangle = \frac{1}{|\Omega|}\int_\Omega \cdot\,\mathrm{d}v\,, \qquad \langle\cdot\rangle^\Gamma = \frac{1}{|\Gamma|}\int_\Gamma \cdot\,\mathrm{d}s \tag{25}
$$

Instead of the standard volume averaging approach (Whitaker 1998), that involves either a moving average or a local kernel, since we are now only interested in the upscaled particulate processes, we can simply apply this static volume averaging to , obtaining:

$$
\begin{aligned}
&\partial_t\langle f\rangle + \langle \mathrm{Pe}\nabla\cdot(\boldsymbol{v}f) - D\Delta f\rangle = \langle B_1(f,\ell)\rangle\\
&+\sum_X \mathrm{Da}_\mathrm{X}\left(\left\langle A_X^+(f,f,\ell)\right\rangle + \left\langle A_X^-(f,f,\ell)\right\rangle + \langle B_X(f,f,\ell)\rangle\right)
\end{aligned} \tag{26}
$$

where we have to remember that f and all the kernels are functions of space and particle size, and therefore they all give rise to closure problems.

Applying the divergence theorem, the second and third terms on the lhs of Eq. 26 can be rewritten as:

$$
\begin{aligned}
\langle \mathrm{Pe}\nabla\cdot(\boldsymbol{v}f) - D\Delta f\rangle &= \langle \nabla\cdot(\mathrm{Pe}\boldsymbol{v}f - D\nabla f)\rangle\\
&= \frac{|\Gamma|}{|\Omega|}\langle \boldsymbol{n}\cdot(\mathrm{Pe}vf - D\nabla f)\rangle^\Gamma + \frac{1}{|\Omega|}\int_{\partial\Omega}\boldsymbol{n}\cdot(\mathrm{Pe}vf - D\nabla f)\,\mathrm{d}s\\
&= \frac{|\Gamma|}{|\Omega|}\langle C(f,\delta)\rangle^\Gamma + \frac{1}{|\Omega|}\mathfrak{F}
\end{aligned} \tag{27}
$$

where $\frac{1}{|\Omega|}$ is the pore specific surface area, $\partial\Omega$ are the external REV boundaries and $\mathfrak{F}$ are the total fluxes through them. The upscaling problem, assuming a macroscopic equilibrium (steady state) configurations, consists in finding an approximation for

$$\mathfrak{F} = \langle B_1(f,\ell)\rangle + \sum_X \mathrm{Da}_X\left(\left\langle A_X^+(f,f,\ell)\right\rangle + \left\langle A_X^-(f,f,\ell)\right\rangle + \langle B_X(f,f,\ell)\rangle\right) - \frac{|\Gamma|}{|\Omega|}\langle C(f,\delta)\rangle^\Gamma$$

as a function of macroscopic variable $\langle f\rangle$ and appropriate macroscopic effective parameters. This is tackled in homogenisation (Hornung 1991) and volume averaging theory (Whitaker 1998) by expanding the variable f as $f = \phi\langle f\rangle + \phi\mathbf{w}\cdot\nabla f$, where ϕ is a function needed to decouple fast reactions, neglected (it tends to one) in the standard upscaling for slow reactions, and $\mathbf{w}$ is given by a local cell problem. This approach, however, in case of nonlinear terms, leads to ϕ, $\langle f\rangle$ and $\mathbf{w}$ being coupled.

4.2 Upscaling of Particle Linear Processes

In this section we specialise our discussion to shear-induced linear events only, leaving the detailed analysis of the other terms in Eq. 26 for future works. Among all the possible events described in Sect. 3.3, the only linear ones are the deposition (when k_c does not depend on f) and the single-particle breakage (see Eq. 19).

To avoid solving the PDE in the five-dimensional space, we focus on steady state solutions and on a single particle size. In general, however, a breakage of a particle of size ℓ generates smaller particles and these have a finite probability of undergoing another breakage event. This results in a one-way coupled cascade of equations where, to solve for particles of size ℓ we first need to solve for all larger particles. However, we can neglect this coupling if one of the following assumptions hold:

- The initial distribution (i.e., the inlet distribution for steady state problems) is concentrated around a single particle size which, having neglected aggregation, represents the largest possible size which is therefore fully decoupled from the others.
- The breakage frequencies are small enough to assume that, in a single REV, each particle can undergo only one breakage event during its residence time.
- The daughter distribution function $\mathcal{A} = 0$, i.e., particles are removed from the system (or no longer tracked) once they break. This is a common approach for estimating the frequency of shear-induced events without tracking the subsequent particle dynamics (Saha et al. 2016).

Therefore, to upscale the breakup due to shear with a bottom up approach, we fix a single particle size and we can then study the behaviour of a *mono-dispersed* sample of particles. Although it is important to stress that the behaviour of a poly-dispersed population is not the trivial superimposition of mono-dispersed particle dynamics, this assumption reduces the complexity of the system allowing us to focus on the role of shear heterogeneity on breakage phenomena. We therefore consider the simplified version of Eq. 24

$$\frac{\partial f}{\partial t} + \mathrm{Pe}\,\nabla\cdot(\boldsymbol{v}f) - D\Delta f = -\mathrm{Da}_\beta \beta f\,, \tag{28}$$

where f can now be interpreted as the concentration of particles of mass m.

It is important to notice, however, that, when the assumptions above are relaxed, particles smaller than ℓ will have an extra source term coming from breakage of larger particles. As we will see later, this is a heterogeneous term, which will further generate heterogeneous spatial distributions, affecting significantly deposition but also dispersion properties.

The upscaling of deposition phenomena is a widely studied problem (Boccardo et al. 2017; Elimelech et al. 1995; Krehel et al. 2015; Boccardo et al. 2019). While the same approaches could be used here to include deposition, we focus here on the heterogeneous shear-driven reaction term and therefore assume a Neumann no-flux boundary condition:

$$\boldsymbol{n} \cdot (\mathrm{Pe}\, \boldsymbol{v} f - D \nabla f) = 0 \,. \tag{29}$$

Applying the averaging described above to eqs. 29 and 28 we seek a macroscopic representation of the type

$$\mathfrak{F} = -\left\langle \mathrm{Da}_\beta \beta f \right\rangle = -\langle \mathrm{Da}_{\mathrm{mi}} f \rangle \approx -\mathrm{Da}_{\mathrm{Ma}} \langle f \rangle = \mathrm{Da}_{\beta,\mathrm{Ma}} \beta_{\mathrm{Ma}} \langle f \rangle \,, \tag{30}$$

where β, as defined in Eq. 6, is the breakage kernel and depends on shear (and therefore space $\boldsymbol{x}$, see Eq. 8) and particle size ℓ. A summary of the explicit definition of β and Da_β is reported in table 2. Having fixed here the size ℓ (through the mass m), we can include it in an overall pore-scale reaction constant, $\mathrm{Da}_{\mathrm{mi}} = \mathrm{Da}_\beta\, \beta(\ell)$. In Eq. 30, we have assumed the existence of an "effective" linear macro-scale reaction rate $\mathrm{Da}_{\mathrm{Ma}}$ which depends on the particle size and describes the effects observed at the macro-scale obtained by this particular mechanism. This macroscopic reaction constant can then be split (similarly to what we have done in Eq. 30) into the product of a macroscopic breakage kernel β_{Ma} , which carries all the dependencies of particle size (and is equal to one for the reference particle of size $\mathfrak{l}$), and a breakage macroscopic constant $\mathrm{Da}_{\beta,\mathrm{Ma}}$[2].

There are several methods to numerically compute the macroscopic reaction rate. In this case, for example, it is possible to evaluate directly the spatial average of the term $\langle \beta f \rangle$. However, we applied here a more general approach, which is valid also for deposition and the presence of more than one micro-scale phenomena at the same time. Using Eq. 27 and the hypothesis of lateral periodicity, we can, in fact, compute $\mathfrak{F}$ by evaluating the inlet and outlet fluxes of Eq. 28 as follows:

$$\mathrm{Da}_{\mathrm{Ma}} = \frac{1}{\langle f \rangle} \int_{\partial\Omega} \boldsymbol{n} \cdot (\mathrm{Pe}\, \boldsymbol{v} f - D \nabla f)\, \mathrm{d}s \tag{31}$$

The macroscopic reaction constant $\mathrm{Da}_{\mathrm{Ma}}$, for a fixed a velocity field $\boldsymbol{v}$ and a reaction kernel β, is therefore a function of only two terms: $\frac{\mathrm{Pe}}{D}$ and $\frac{\mathrm{Da}_\beta\, \beta}{D}$, which can be directly linked to the particle size ℓ.

From the practical point of view, Eq. 31 has to be computed on a non-trivial stationary solution of . This exists only when a concentration gradient is imposed at the boundaries[3]. The assumption of constant concentration in the inlet often used, however, is not a good representation of the asymptotic REV, so quasi-periodic BCs are here used (Boccardo et al. 2018, 2017). Then, volumetric and surface integrals in Eq. 31 have to be extracted. In some cases, these can introduce cancellation and numerical errors due to the fact that, when the reaction rate is high, the average $\langle f \rangle$ vanishes. A convenient alternative is to compute the effective reaction rate $\mathrm{Da}_{\mathrm{Ma}}$ as the first smallest eigenvalue of the differential operator

[2] This splitting is necessary to reobtain, at the macroscale, an equation of the same form of the micro-scale one. Although this is not explicitly performed here, this splitting is trivial and always possible. The evaluation of the $\mathrm{Da}_{\mathrm{Ma}}$ for particles of size $\mathfrak{l}$ gives the reference $\mathrm{Da}_{\beta,\mathrm{Ma}}$, and the macroscopic kernel β_{Ma} dependent on the particle size is simply obtained as $\frac{\mathrm{Da}_{\mathrm{Ma}}}{\mathrm{Da}_{\beta,\mathrm{Ma}}}$.

[3] In fact, simply assuming periodic boundary condition would result in a trivial stationary solution equal to zero everywhere.

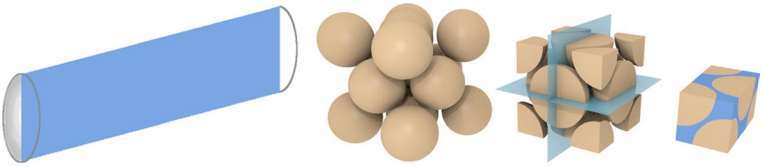

Fig. 2 Sketch of the two-dimensional channel (figure on the far-left) and FCC packing domains with shown the cut performed to obtain the final domain used in the simulation (figure on the far-right)

(Allaire and Raphael 2007; Mauri 1991; Municchi and Icardi 2020), under periodic (or Neumann) external boundary conditions which represents the macroscopic effective reaction rate. Our future works will explore more in details this approach for various physical problems. This is used here only as a comparison for the channel flow example in the next section.

Two-particle processes could be similarly studied in the assumption that the second particle j has a fixed size ℓ_j and its concentration field is constant. This can be also thought as a linearisation, assuming that the concentration of particle of size ℓ_j changes at a much slower speed. A proper nonlinear generalisation and perturbation approaches will be studied in future works.

5 Numerical Examples

In this section we apply the framework derived previously (in particular in Sect. 4.2) to different example problems to show the potentiality of the whole approach.

Two different geometries were chosen: a two-dimensional channel (CH) with an aspect ratio of 5 and a three-dimensional face-centered cubic domain (FCC) with porosity of 40%, as depicted in Fig. 2. A Cartesian orthonormal reference frame is used, both for the CH geometry, $\{O, \mathbf{e}_x, \mathbf{e}_y\}$, and the FCC geometry, $\{O, \mathbf{e}_x, \mathbf{e}_y, \mathbf{e}_z\}$, where O is the origin and $\mathbf{e}_x$ is the unit vector parallel to the main flow direction. Given the symmetry of the FCC packing (Crevacore et al. 2016; Boccardo et al. 2017), just one fourth of the cubic structure was discretised and used for simulation purposes. All simulations are performed with the OpenFOAM® finite-volumes open-source library.

For each geometry, first Stokes equation (Eq. 1) is solved assuming periodic boundary conditions on the external boundaries of the domain and no slip condition on the solid walls, i.e., the lateral boundaries of the CH, and on the grain surface of the FCC. To drive the flow, a pressure drop between inlet and outlet boundaries, such that the resulting velocity has a unitary spatial average, i.e., $\langle v \rangle = 1$, in both geometries. With these inputs, we obtain a fully developed parabolic flow within the channel. The contour plots of the velocity and the shear in the FCC is instead reported in Fig. 3.

The integro-partial differential equation Eq. 24 which represents the full population balance model is commonly solved using two approaches, the quadrature-based method of moments (QMOM) (McGraw 1997) and the method of classes (Kumar and Ramkrishna 1996). These two methods allow the resolution of the general PBE including all the particle evolution mechanisms needed for the particular application (e.g., the different kernels we described in appendix 3). In the QMOM (or more in general moment-based methods) the resolution of the PBE is obtained by replacing it with a set of transport equations for the lower order statistical moments of the PSD. Several variants of the QMOM were proposed

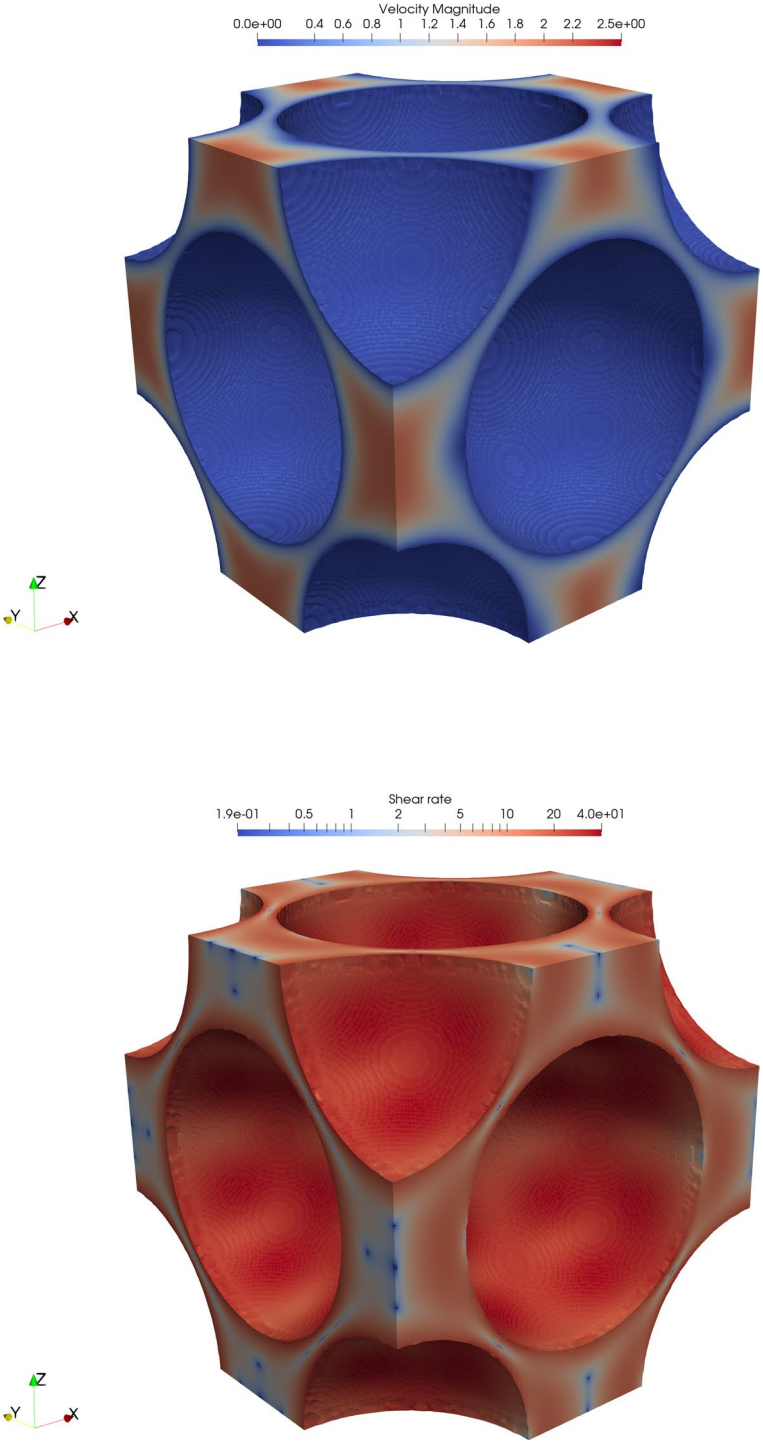

Fig. 3 Contour plot of the velocity (top) and shear (bottom) in the FCC system

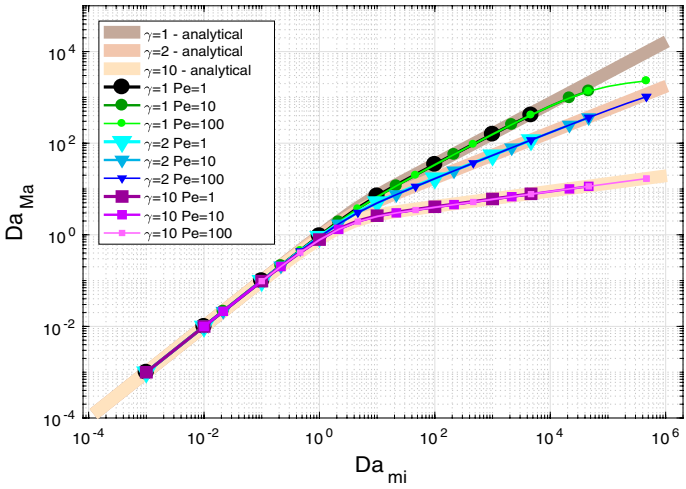

Fig. 4 Two-dimensional channel: macro- vs. micro-scale Damköhler numbers for different γ and Pe. We also report as comparison the analytical law extracted in eqs. 32and 33 for the same values of γ

to address some of the drawbacks of this approach, such as the Direct QMOM (Marchisio and Fox 2005), Extended QMOM (Yuan et al. 2012), Conditional QMOM (Yuan and Fox 2011). In the method of classes, instead, the PSD is represented by a discrete number of sizes and a set of transport equations for each class is obtained. We refer for a more complete overview of such models to (Marchisio and Fox 2013).

The QMOM and the method of classes for a general solution of the PBE are readily available in OpenFoam (Lehnigk et al. 2021). In this work, however, the solution of the PBE transport equation, under the hypothesis considered here, Eq. 28, reduces to the solution of a simple linear advection diffusion equation with appropriate heterogeneous reaction terms, therefore, an ad-hoc transport equation is implemented.

Here, we present a parametric analysis obtained by considering different values of the γ exponent in the breakage kernel (see eqs. 6and 7 and Eq. 9 with $\gamma' = 0$), and of the Péclet number. In particular, for the parameter γ we have considered:

- $\gamma = 1$ to study the linear dependence of the reaction coefficient on the shear rate;
- $\gamma = 2, 3, 10$ to investigate a power law of the share rate.

Whereas for the Péclet number, in the form of overall Péclet number: Pe/D, we considered a range of values between 10^{-2} and 10^{2}. In the rest of this work, in order to use a lighter notation, we will use the symbol Pe to indicate the overall Péclet number. All the results shown in the next sections must be intended with the diffusion coefficient implied in the definition of the Pe. We recall, in fact, that, even in the dimensionless formulation, particles of different sizes can have different diffusion coefficients as well as different reaction constant (breakage kernels).

Finally, for each combination of Pe and γ, we assigned a broad range of values for the breakup reaction constant $\mathrm{Da}_{\mathrm{mi}}$ (which was defined in). This dimensionless formulation allows us to run the whole set of simulations varying only three parameters $\gamma, \mathrm{Pe}, \mathrm{Da}_{\mathrm{mi}}$ and subsequently remap the results and study the dependencies on the internal parameters ℓ, Pe, D and the other dimensionless groups appearing in the Damköhler numbers (see

Table 2). After reaching steady state, integration Eq. 30 gives a macro-scale effective reaction rate as a function of the above parameters. More details of the computational setup and numerical schemes are reported in previous works (Boccardo et al. 2020).

5.1 The Two-Dimensional Channel

We start our analysis of the results by reporting in Fig. 4 the macroscopic Damköhler number as function of the microscopic one, for all the different operating conditions we considered in this work.

Under the chosen parametrisation, two different trends can be highlighted. For small values of $\mathrm{Da}_{\mathrm{mi}}$, to which correspond small frequencies β_0, the equivalent macroscopic reaction rates $\mathrm{Da}_{\mathrm{Ma}}$ collapse on a single curve due to the dimensional scaling. This is due to the slow reaction kinetics that, although heterogeneous, is quickly homogenised by diffusion. On the other and, at higher breakage frequencies, (i.e. high values of $\mathrm{Da}_{\mathrm{mi}}$) a strong dependence on the shear exponent γ appears evident.

For the two-dimensional channel we can observe that there is no dependence on the Péclet number of the results. This is due to the pathological nature of the channel flow where mixing is purely due to lateral diffusion. However, despite being a simplified case, channel flows are the phenomenological basis for more complex porous media mixing structures (Dentz et al. 2018).

From the results shown in Fig. 4, the dependence of the macroscopic breakup rate is well described by:

$$\mathrm{Da}_{\mathrm{Ma}} \sim \mathrm{Da}_{\mathrm{mi}}\,, \qquad \text{for } \mathrm{Da}_{\mathrm{mi}} < 1\,, \tag{32}$$

$$\mathrm{Da}_{\mathrm{Ma}} \sim \mathrm{Da}_{\mathrm{mi}}^{\frac{2}{\gamma+2}}\,, \qquad \text{for } \mathrm{Da}_{\mathrm{mi}} > 1\,, \tag{33}$$

where the dependence on the particle size is implicitly taken into account by $\mathrm{Da}_{\mathrm{mi}}$ by its dependence on the breakage kernel (see Eq. 30) and on the diffusion coefficient. This latter effect is compatible with the fact that, when reaction events (i.e. the breakage events) are faster then diffusion, the system enters in a mixing-limited regime where a nonlinear dependence of the macro-scale reaction on the micro-scale breakage frequency is expected. However, contrarily to surface reactions (Boccardo et al. 2017)

This dependence is thus well characterised as a power-law, where the controlling parameter is the shear rate exponent γ.

This evidence is confirmed, in turn, by semi-analytical reference results. As explained in the previous section and in (Municchi and Icardi 2020), we can solve an eigenvalue problem for the micro-scale cell problem with periodic inlet/outlet boundary conditions. For a channel, this results in solving only in the direction of the channel cross-section (here assumed $[-1, 1]$) and extracting the effective reaction rate by computing the principal eigenvalue. Substituting the breakage kernel in Eq. 9 and computing the shear rate in the channel, this can be rewritten in the form of a Generalised Airy Equation for a half-channel:

$$\begin{aligned} &f''(y) - \beta_0(\gamma+1)y^{\gamma}f(y) = \lambda f(y) && \text{in } [0,1] \\ &f'(y) = 0 && \text{on } y = 0, y = 1, \end{aligned} \tag{34}$$

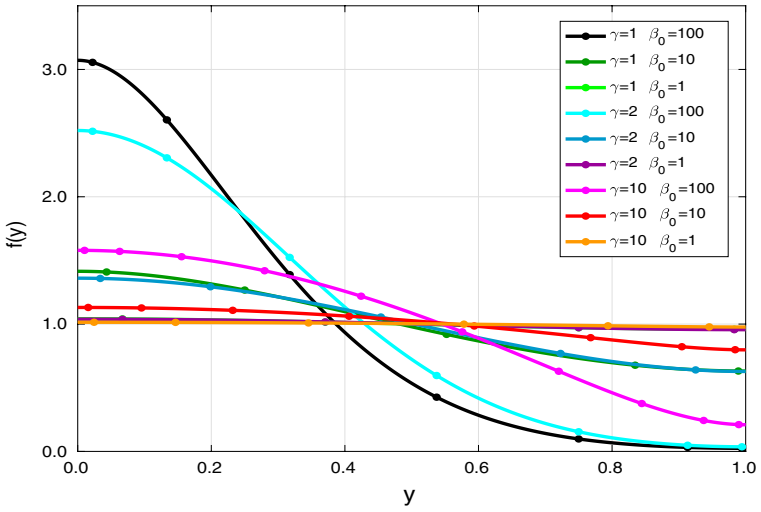

Fig. 5 Semi-analytical stationary concentration profiles for the Two-dimensional channel or different γ and Pe

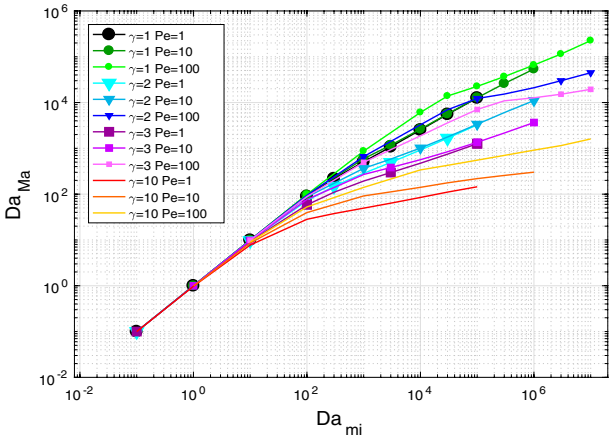

Fig. 6 FCC packing: macro- vs. micro-scale Damköhler numbers

where $\beta_0(\gamma+1)y^\gamma$ is the breakage kernel. We remind here that this cell problem only represents the asymptotic (equilibrium) limit and not the transient Taylor dispersion. Equation 34 is solved with high-resolution spectral methods with the Chebfun Driscoll et al. (2014) package. The eigenvalue λ represents the effective homogeneous reaction that counterbalance the heterogeneous shear-induced events (Fig. 5).

5.2 The FCC Packing

For a more complex three-dimensional FCC packing, as long as the process is diffusion controlled or the breakage frequency is relatively small, the linear relation between the

micro-scale Damköhler and the macro-scale rate is recovered (similar to one shown in Fig. 4), as shown in Fig. 6.

However, increasing the pore-scale breakage frequency, the results for this more realistic case are more complex that the ones presents for the CH system. In particular, we can identify the following new features which were not present in Fig. 4: *i*) the transition from linear to power-law dependence spans a broader range of $\mathrm{Da}_{\mathrm{mi}}$ values with respect the two-dimensional channel, and it becomes more difficult to identify an asymptotic trend for each γ; *ii*) for $\mathrm{Da}_{\mathrm{mi}} >> 1$ a dependence on the Péclet number appears, and we can qualitatively infer from Fig. 6 that this dependence increases with γ. The exact functional dependence in this case would be a two-dimensional function of the microscopic Damköhler and the Péclet : $\mathrm{Da}_{\mathrm{Ma}} = \mathrm{Da}_{\mathrm{Ma}}(\mathrm{Da}_{\mathrm{mi}}, \mathrm{Pe})$ which can be calculated from the data in Fig. 6.

Moreover, we can observe that transition regimes seem to extend up to values of $\mathrm{Da}_{\mathrm{mi}}$ (i.e., $> 10^3$) which are no longer realistic for practical applications. This can be explained in terms of influence of the porous medium structure on the reaction/transport phenomena. The dependence on the Péclet number seems to be larger for large values of γ with a behaviour similar to the channel presented in the previous case when $\gamma = 1$. The values of $\mathrm{Da}_{\mathrm{mi}}$ for which we have the switch from the linear to the nonlinear behaviour has a dependence on γ and Pe and the switch happen at smaller $\mathrm{Da}_{\mathrm{mi}}$ number as the γ and Pe increase. This behaviour can at least intuitively explained in terms of influence of the porous medium structure on the reaction/transport phenomena. The higher is γ the more heterogeneous is the reacting front, and the greater is the disturbance produced by the presence of the grains (while a sharper front would channelling through the medium more easily).

The asymptotic behaviour with respect to γ, discovered for the channel, seems to persist also in this geometry, in particular for small Pe, while no definitive conclusions can be drawn for larger Pe which could also be more sensitive to numerical errors. Regardless of the geometry of the medium, the limiting case of $\gamma \to \infty$ is expected to behave like non-premixed combustion (in the mixing limited limited) and perfect deposition, where the reaction happens on a two-dimensional manifold only, and $\mathrm{Da}_{\mathrm{Ma}}$ reaches a Pe-dependent flat value.

6 Conclusions

In this work we present a model for particulate flows based on the Population Balance Equation (PBE) framework with specific consideration for micro-fluidics and porous media problems. We first introduce a novel dimensional analysis of the PBE including a new term describing breakup after particle-particle collisions. We then focus on upscaling and the definition of averaged PBE kernels in heterogeneous flows. Describing the particle dynamics and evolution in micro-scale complex geometries, in fact, has enormous potential in a wide range of industrial and environmental applications, but also presents challenges which make such systems extremely interesting and at the same time extremely difficult to model. These include the prohibitive computational cost of fully resolved simulation and the need of macro/Darcy/continuum-scale models. The averaging operation, however, introduces additional coupling between the different particulate processes and between particles of different sizes. After describing a general upscaling framework we limit the discussion to first-order shear-induced events, in particular the breakage of particles inside the pores. We show how the shear-induced breakage can be considered as a linear process in

the concentration of the particles and we derived the relevant dimensionless quantities to describe it at the pore- and macro-scales. To test our framework in numerical experiments, we consider a two-dimensional channel, where simplified one-dimensional results can be obtained, and a three-dimensional periodic porous medium made of a Face-Centred packing of spheres.

We show that the upscaling procedure follows the expected behaviour, with the macroscopic breakage frequencies loosing the linear dependence with respect to its pore-scale analogue, due to the limited mixing. We also show the effect of the heterogeneity which is controlled by the exponent of the shear-induced breakage kernel. For the two-dimensional channel we propose a law for macroscopic effective reaction rate based on the pore-scale rate and the shear exponent. This qualitatively is reproduced also for more complicated system, like the sphere packing, but with a more complex dependence of the Péclet number.

This work represents a first attempt towards the systematic upscaling of the PBE framework in periodic porous media. Future work currently under development include the upscaling of nonlinear processes as well as the interaction between particulate processes and deposition.

Funding This research has been funded by the Royal Academy of Engineering (Asphaltene dynamics at the pore-scale and the impact on oil production at the field-scale IAPP 18-19 285).

Data Availability and Material The data that support the findings of this study are available from the corresponding author upon reasonable request.

Code Availability The code is available from the corresponding author upon reasonable request.

Declarations

Conflict of interest The authors assert that there is no conflict of interest in any aspect related to their submission of this work.

Consent to participate Not available.

Consent to publication Not available.

Ethical approval Not available.

References

Allaire, G., Raphael, A.-L.: Homogenization of a convection-diffusion model with reaction in a porous medium. C.R. Math. **344**, 523 (2007)

Auriault, J.L., Adler, P.M.: Taylor dispersion in porous media: analysis by multiple scale expansions. Adv. Water Resour. **18**, 217 (1995)

Barthelmes, G., Pratsinis, S.E., Buggisch, H.: Particle size distributions and viscosity of suspensions undergoing shear-induced coagulation and fragmentation. Chem. Eng. Sci. **58**, 2893 (2003)
Bedrikovetsky, P.: Upscaling of stochastic micro model for suspension transport in porous media. Transp. Porous Media **75**, 335 (2008)
Bird, R., Stewart, W., Lightfoot, E.: Transport Phenomena. John Wiley & Sons Inc, New York (2002)
Boccardo, G., Crevacore,E., Passalacqua, A., Icardi, M.: Computational analysis of transport in three-dimensional heterogeneous materials: an OpenFOAM-based simulation framework. Comput. Vis. Sci. **23** (2020)
Boccardo, G., Crevacore, E., Sethi, R., Icardi, M.: A robust upscaling of the effective particle deposition rate in porous media. J. Contam. Hydrol. **212**, 3 (2017)
Boccardo, G., Sokolov, I.M., Paster, A.: An improved scheme for a robin boundary condition in discrete-time random walk algorithms. J. Comput. Phys. **374**, 1152 (2018)
Boccardo, G., Sethi, R., Marchisio, D.L.: Fine and ultrafine particle deposition in packed-bed catalytic reactors. Chem. Eng. Sci. **198**, 290 (2019)
Buffo, A., Vanni, M., Marchisio, D.: Multidimensional population balance model for the simulation of turbulent gas-liquid systems in stirred tank reactors. Chem. Eng. Sci. **70**, 31 (2012)
Chen, S., Li, S.: Collision-induced breakage of agglomerates in homogenous isotropic turbulence laden with adhesive particles. J. Fluid Mech. **902** (2020)
Crevacore, E., Boccardo, G., Marchisio, D., Sethi, R.: Microscale colloidal transport simulations for groundwater remediation. Chem. Eng. Trans. **47**, 271 (2016)
Dentz, M., Icardi, M., Hidalgo, J.J.: Mechanisms of dispersion in a porous medium. J. Fluid Mech. **841**, 851 (2018)
Di Pasquale, N., Marchisio, D., Barresi, A.: Model validation for precipitation in solvent-displacement processes. Chem. Eng. Sci. **84**, 671 (2012)
Di Pasquale, N., Marchisio, D.L., Carbone, P., Barresi, A.A.: Identification of Nucleation Rate Parameters with MD and validation of the CFD Model for Polymer Particle Precipitation. Chem. Eng. Res. Des. **91**, 2275 (2013)
Di Pasquale, N., Marchisio, D.L., Barresi, A.A., Carbone, P.: Solvent structuring and its effect on the polymer structure and processability: the case of water-acetone poly-ε-caprolactone mixtures. J. Phys. Chem. B **118**, 13258 (2014)
Driscoll, T.A., Hale, N., Trefethen, L.N.: Chebfun Guide. Pafnuty Publications. (2014) http://www.chebfun.org/docs/guide/
Elimelech, M., Gregory, J., Jia, X., Williams, R.: Particle Deposition & Aggregation. Butterwort-Heinemann, Oxford (1995)
Ferry, J., Rani, S.L., Balachandar, S.: A locally implicit improvement of the equilibrium Eulerian method. Int. J. Multiph. Flow **29**, 869 (2003)
Frungieri, G., Vanni, M.: Aggregation and breakup of colloidal particle aggregates in shear flow: a combined Monte Carlo–Stokesian dynamics approach. Powder Technol. **388**, 357 (2021)
Frungieri, G., Babler, M.U., Vanni, M.: Shear-induced heteroaggregation of oppositely charged colloidal particles. Langmuir **36**, 10739 (2020)
Grigoriev, V.V., Iliev, O., Vabishchevich, P.N.: Computational identification of adsorption and desorption parameters for pore scale transport in periodic porous media. J. Comput. Appl. Math. **370**, 112661 (2020) https://www.sciencedirect.com/science/article/pii/S0377042719306661
Hornung, U.: Homogenization and Porous Media. Springer, New York (1991)
Icardi, M., Dentz, M.: Probability density function (PDF) models for particle transport in porous media. GEM Int. J. Geomath. **11**, 1 (2020)
Khalifa, A., Breuer, M.: An efficient model for the breakage of agglomerates by wall impact applied to Euler–Lagrange LES predictions. Int. J. Multiph. Flow **142**, 103625 (2021)
Krehel, O., Muntean, A., Knabner, P.: Multiscale modeling of colloidal dynamics in porous media including aggregation and deposition. Adv. Water Resour. **86**, 209 (2015). https://doi.org/10.1016/j.advwatres.2015.10.005
Kumar, S., Ramkrishna, D.: On the solution of population balance equations by discretization–I: a fixed pivot technique. Chem. Eng. Sci. **51**, 1311 (1996)
Lattuada, M., Zaccone, A., Wu, H., Morbidelli, M.: Population-balance description of shear-induced clustering, gelation and suspension viscosity in sheared DLVO colloids. Soft Matter **12**, 5313 (2016)
Lavino, A.D., Di Pasquale, N., Carbone, P., Marchisio, D.L.: A novel multiscale model for the simulation of polymer flash nano-precipitation. Chem. Eng. Sci. **171**, 485 (2017)

Lehnigk, R., Bainbridge,W., Liao, Y., Lucas, D., Niemi, T., Peltola, J., Schlegel, F.: An open-source population balance modeling framework for the simulation of polydisperse multiphase flows, AIChE Journal p. e17539 (2021)
Marcato, A., Boccardo,G., Marchisio, D.: A computational workflow to study particle transport and filtration in porous media: Coupling CFD and deep learning. Chem. Eng. J. **417**, 128936 (2021), ISSN 1385-8947, https://www.sciencedirect.com/science/article/pii/S1385894721005295
Marchisio, D., Fox, R.: Solution of population balance equations using the direct quadrature method of moments. J. Aerosol Sci. **36**, 43 (2005)
Marchisio, D.L., Fox, R.O.: Computational Models for Polydisperse Particulate and Multiphase Systems. Cambridge University Press, Cambridge (2013)
Mauri, R.: Dispersion, convection, and reaction in porous media. Phys. Fluids A **3**, 743 (1991)
McGraw, R.: Description of aerosol dynamics by the quadrature method of moments. Aerosol Sci. Tech. **27**, 255 (1997)
Municchi, F., Boccardo,G., Tartakovsky, D., Icardi, M.: Macroscopic models for fast reaction and adsorption in porous media,in preparation (-)
Municchi, F., Icardi, M.: Generalized multirate models for conjugate transfer in heterogeneous materials. Phys. Rev. Res. **2**, 013041 (2020)
Nassar, N.N., Betancur, S., Acevedo, S., Franco, Cortés, F.B.: Development of a population balance model to describe the influence of shear and nanoparticles on the aggregation and fragmentation of asphaltene aggregates. Ind. Eng. Chem. Res. **54**, 8201 (2015)
Passalacqua, A., Icardi, M., Madadi, E., Bachant, P., Hu, X., Heylmun, J., Weaver, J.: *OpenQBMM*, https://zenodo.org/record/5803026
Patzek, T.W.: *Description of Foam Flow in Porous Media by the Population Balance Method* Surfactant-Based Mobility Control, pp. 326–341, https://pubs.acs.org/doi/abs/10.1021/bk-1988-0373.ch016 (1988)
Ramkrishna, D.: Population Balances. Academic Press, San Diego (2000)
Sadegh-Vaziri, R., Ludwig, K., Sundmacher, K., Babler, M.U.: Mechanisms behind overshoots in mean cluster size profiles in aggregation-breakup processes. J. Colloid Interface Sci. **528**, 336 (2018)
Saha, D., Babler, M.U., Holzner, M., Soos, M., Lüthi, B., Liberzon, A., Kinzelbach, W.: Breakup of finite-size colloidal aggregates in turbulent flow investigated by three-dimensional (3D) particle tracking velocimetry. Langmuir **32**, 55 (2016)
Seetha, N., Raoof, A., Kumar, M.M., Hassanizadeh, S.M.: Upscaling of nanoparticle transport in porous media under unfavorable conditions: Pore scale to Darcy scale. J. Contam. Hydrol. **200**, 1 (2017)
Serra, T., Casamitjana, X.: Effect of the shear and volume fraction on the aggregation and breakup of particles. AIChE J. **44**, 1724 (1998)
Serra, T., Colomer, J., Casamitjana, X.: Aggregation and breakup of particles in a shear flow. J. Colloid Interface Sci. **187**, 466 (1997)
Solsvik, J., Tangen, S., Jakobsen, H.A.: On the constitutive equations for fluid particle breakage. Rev. Chem. Eng. **29**, 241 (2013)
Vanni, M.: Approximate population balance equations for aggregation-breakage processes. J. Colloid Interface Sci. **221**, 143 (2000)
Whitaker, S.: The Method of Volume Averaing. Springer Science & Business Media, Cham (1998)
Won, J., Lee, J., Burns, S.E.: Upscaling polydispersed particle transport in porous media using pore network model. Acta Geotech. **16**, 421 (2021)
Yuan, C., Fox, R.O.: Conditional quadrature method of moments for kinetic equations. J. Comput. Phys. **230**, 8216 (2011)
Yuan, C., Laurent, F., Fox, R.: An extended quadrature method of moments for population balance equations. J. Aerosol Sci. **51**, 1 (2012)
Zitha, P.L.J., Du, D.X.: A new stochastic bubble population model for foam flow in porous media. Transp. Porous Media **83**, 603 (2010)